Agrociencia

FUNCTIONAL STABILITY OF THE INVERTED PENDULUM AND ITS RELATION TO UNCREWED AERIAL VEHICLE WINGS THROUGH SYSTEM MATHEMATICAL MODELING AND SIMULATION

Naji Mordi Naji **Al-Dosary**[1*], Alex Greg **Zolotorevskiy**[2], Cassidy Paul **Schram**[2]

[1] King Saud University. College of Food and Agriculture Sciences. Department of Agricultural Engineering. Riyadh, Saudi Arabia.
[2] University of Florida. Department of Mechanical and Aerospace Engineering. Gainesville, FL, USA.
* Author for correspondence: nalsawiyan@ksu.edu.sa

Citation: Al-Dosary NMN, Zolotorevskiy AG, Schram CP. 2023. Functional stability of the inverted pendulum system and its relation to uncrewed aerial vehicle wings through mathematical modeling and simulation of the system. **Agrociencia.** doi.org/ 10.47163/agrociencia.v57i8.2956

Editor in Chief:
Dr. Fernando C. Gómez Merino

Received: January 28, 2023.
Approved: July 26, 2023.
Published in Agrociencia: December 13, 2023.

This work is licensed under a Creative Commons Attribution-Non- Commercial 4.0 International license.

ABSTRACT

The flight instability of an uncrewed aerial vehicle (UAV) can be considered critical, and investigations of stability can be compared to the study of the stabilization of an inverted pendulum. This study investigated the stability of two dynamic systems, represented by an inverted pendulum and a simple approximation of an aircraft wing surface exposed to aerodynamic forces. This study illustrates the advantages of time-domain simulation for solving the differential equation of motion. The simulation used the Euler integration approach for various system parameters. Essentially, an aircraft in flight must constantly maintain pitch stability, which, in practical considerations, can be compared to the mechanism of a rotary motion represented by the up-swinging motion of an inverted pendulum. The pendulum may conserve the same concept as an aircraft's acceleration, as both are affected by the same gravity and acceleration forces, in which the longitudinal stability of the aircraft must be ensured immediately upon takeoff. An inverted pendulum and a UAV aircraft system simulation were developed with basic MATLAB software. The inverted pendulum simulation showed that as the value of the spring's stiffness at the limit of stability (k_{lim}) increased, the system became more convergent and, as a result, more stable. The stiffness of the spring at the limit of stability, k_{lim} = 32.69 N m^{-1} (i.e., equivalent to an initial angular rotation $\theta = 5$ °), and the system's stability were observed up to the value of k_{lim} = 179.79 N m^{-1}, which resulted in an unstable short initial period. In addition, for the aircraft's wing, the damping coefficient (c_{lim}) value was in the range of $c_{lim} \geq$ 10,000 N s m^{-1}. Therefore, with the damping ratio ζ being equal to zero, the system vibrated consistently at its natural frequency (w_n), never deviating drastically to become unstable.

Keywords: Aerodynamic forces, aircraft wings, damping coefficient, Euler integration, limiting spring stiffness.

INTRODUCTION

An overview of the scientific pendulum scheme

A pendulum rotating around a pivot point, whether suspended or inverted, includes a long rigid arm that ends with a mass affected by gravity at various time intervals and rotation angles. Studying the time period that the pendulum takes to become stable is one of the most important variables to be taken into consideration when analyzing the effects of vibration in numerous mechanical applications, including agricultural machinery. In the agricultural field, it is also possible to compare the effect of forces on the movement and acceleration of a pendulum with the effect of forces and acceleration on the stability of the center of gravity (CG) of a farm tractor to predict and prevent the tractor rolling over. An oscillation methodology for tractors is easily applied to find the height of the center of gravity (CG) of agricultural tractors, where a vertical plane containing the center of gravity is obtained by measuring the relative height levels of the tractor's wheels (Fabbri and Molari, 2004; Khorsandi *et al*., 2018; Bietresato and Mazzetto, 2019).

The concept of a simple pendulum can be illustrated by the seat's shock absorbers and the longitudinal (x) and lateral (y) axis of the driver's seat of a self-propelled agricultural machine (e.g., tractors, combines, lawn mowers, etc.), as well as the flight stability of an uncrewed aerial vehicle (UAV) with or without an associated load during field operations, which means that the dynamic model is with or without change of parameters, as they are all expected to behave in the same way. The pendulum also appears in the design of robotic arm and leg motions (i.e., to increase the walking efficiency of robots and the associated control of robotic manipulators) or a tree trunk and a canopy shaker machine, where the systems can monitor the inverted pendulum's trajectory in order to stabilize their movements. These agricultural applications widely apply the concept of the equilibrium of the pendulum and mass-spring-damper systems (MSD). Recently, modern agricultural practices, especially in the field of control and precision farming methods, have quickly advanced through the application of various technologies, electronic tools, and programming systems, such as LabVIEW, MATLAB, Arduino Uno, Raspberry Pi, etc. These approaches have become key factors contributing to the increased efficiency of agricultural operations, especially regarding machines that are subjected to high levels of vibrations during only the machines that are not cushioned by the soil or the harvested mass (e.g., potato harvesters).

Moreover, a simulation study of the effectiveness of some proposed pendulum models in stabilizing a robot's walk for agricultural machines was performed by Li *et al.* (2021). They established a trajectory-planning method that achieved flexible, stable, and periodic walking independently for bipedal robots in different virtual circumstances that could be realized in real time using linear and inverted pendulum models. The stability of any mechanical system with respect to vibration depends on several different parameters. For example, the mechanical system of an inverted

pendulum attached to a cart shows that the pendulum can be steady in an inverted position if the cart is stationary or if the cart has a displacement moving at a constant velocity, i.e., it has no further acceleration (University of Michigan, 1997). The inverted pendulum is a common application used in several mechanical systems. When the center of gravity (CG) is higher than its pivot point, an inverted pendulum becomes unstable (Hanada *et al.*, 2019). Also, the pendulum's stability is affected by several parameters, as proposed in this study, such as the mass of the pendulum (m), the length to the pendulum's center of mass (l), and the pendulum's angle from vertical (θ).

Simplifying the concept of the relationship between the inverted pendulum scheme and the stability of uncrewed aircraft

In agricultural applications, an UAV flying at low altitudes may encounter unfavorable winds, which will affect the required flight altitude of the aircraft during field operations. Wind may cause the GPS antenna on top of the UAV to fluctuate, affecting its stability, and it may disable the aircraft or affect its operational systems. Therefore, the vibration of the GPS antenna on the fuselage in such a situation is similar to the vibration of an inverted pendulum.

Sharma *et al.* (2021) noted the many current uses of hybrid uncrewed aircraft with both helicopter and fixed-wing technology in civilian life and analyzed their aerodynamic properties, including enhanced payload capacity. The load capacity (empty weight plus added cargo load weight) and position of the center of gravity (CG) are the important factors influencing flight stability that determine the appropriateness of certain applications of the UAV in agricultural field operations, for example, aerial agricultural spraying operations with agrochemicals. Assuming that the UAV aircraft is acting in a consistent rotation, during a turn, the aircraft might act as a pendulum affected by an external force (i.e., an aerial vehicle can swing, similar to a torsional pendulum). Due to the aircraft's shape, especially the design of the wings, which may be affected by external aerodynamic forces, the displacement of the center of gravity will create a significant rolling motion of the wings around the center of the aircraft's lift. If an aircraft is disturbed, resulting in one wing being in a high position and the other wing in a lower position relative to the neutral point of the lateral axis, the weight of the aircraft's main body acts as a pendulum, bringing the aircraft back to its equilibrium level (FAA, 2016). Aerodynamic variables affecting the aircraft's wing systems can help us predict an optimized design of the airframe and the wing structure.

Estevez *et al.* (2021) proposed a control technique utilized for carrying a pendulum with the lowest possible oscillations for a system consisting of a multi-rotor aircraft that transmits a double pendulum. They indicated that the transmission of a multi-pendulum using an aerial vehicle is perfectly adequate to the latest technology in order to study the transportation of UAV-borne payloads using complicated dynamics

considering the estimation and tuning of UAV dynamic parameters. The stability of an inverted pendulum can be used to model the application in flight conditions of an aircraft subject to various aerodynamic forces, such as spraying crop and soil nutrients and applying pesticides and insecticides for pest and weed control in agriculture, with the objective of determining the system's ability to achieve stability, especially in the initial inflight stabilization period. The controlling parameters of the rotary inverted pendulum can be specified in two vibration modes that result in a wide frequency domain with partly large amplitude vibrations. These conditions of large amplitude should be avoided when setting a time-varying set point (Dolatabad *et al.*, 2022). Gunawan *et al.* (2018) developed a four-engine flight system (flying quadrotor) that stabilized an inverted pendulum. The results showed the optimum response of the output roll angle of the inverted pendulum and demonstrated the ability to control a short period of autonomous flight (5.40 s) with a settling time of 0.80 s and an overshoot of the roll angle of 17 °.

Moreover, Sowjanya and Ramesh (2015) and Jibril *et al.* (2021) indicated that the inverted pendulum system is a typical nonlinear, multivariate, and naturally unstable system. The problem of controlling an inverted pendulum is the fluttering of conventional control systems; since the pendulum system is inherently unstable, the pendulum will not remain upright without external forces (i.e., it is unstable without control). This concept can be applied to the longitudinal stability of an aircraft's fuselage as it relates to wing stability. The aircraft's wings are designed to accomplish safe and balanced flight. When the wings of an aircraft move through the air, the position of the center of the aerodynamic lift force remains at the same point regardless of the change in the attack angle of the airfoil blade, with or without vibration. Gatto (2009) investigated a longitudinal stability information technique derived from a wind tunnel test model, which was set up as a pendulum support rig. A test model was inverted and suspended inside the wind tunnel's roof by a supporting strut with a degree of freedom, which allowed the model to move. An additional gimbal attaching the model to the strut was used to allow the model to freely rotate in pitch, thus simulating a device (pendulum) oriented horizontally in a moving body (the wind tunnel).

Since longitudinal stability denotes stability along the plane's latitudinal axis, the effectiveness of the elevator provides aerodynamic control of the aircraft's pitch angle. Technically, the results for the system's sensitivity and the input parameters showed that the length of the pendulum's rod and the pendulum's velocity, mass, inertia, rod angle, and angle of attack had the greatest influence on the estimated values of the magnitude of the pendulum's movement. These parameters can be adjusted to achieve the aircraft's optimum flight performance. As a result, the pendulum model, which has only one degree of freedom, can be referred to as the angular displacement. This angular displacement might act as an unbalanced force, which may cause the stability or instability of the pendulum (Tulapurkara, 2012).

When evaluating the performance of any dynamic model of an UAV, an issue arises concerning the system's control inputs and output states, which can be measured.

However, to take these measurements, an observer is required to estimate the state feedback of the UAV under the influence of an incidental external circumstance. In this simulation study, the stability of two systems was investigated. For example, simulations of an inverted pendulum and a simple approximation of an UAV aircraft's wing were tested for a stable flight of the UAV with a short duration. The study included the development of a time-domain simulation to solve the differential equation of motion. The simulation used the Euler integration approach for various system parameters. The Euler integration approach is a numerical method that gives a value for the displacement, velocity, and acceleration with the time steps for the inverted pendulum and aircraft wing systems. In particular, this is important for cases of interaction between the agricultural apparatus and the material to be processed.

The two systems were investigated by using the simulation program in MATLAB software (The MathWorks Inc., 2022a). Thus, the main objectives of the simulation study were to analyze the motion of a system that included a damper, a spring, and an inverted pendulum. The system needed to be able to maintain the pendulum's stability when it stayed vertical and respond to disturbances to the pendulum's angle and, similarly, disturbances of the angle of attack of the aircraft wing (airfoil) by an aerodynamic force. Thus, to demonstrate the aircraft's flight stability, the simulation should perform in the same way as a stable set of wings symmetrically designed around the center of the longitudinal axis to achieve a suitable attack angle of the aircraft's wings (airfoils) along the lateral axis to obtain an appropriate flight lift level. There is a gap between studies of the concept of a pendulum vibration and the vibration of an UAV aircraft that needs to be adressed. Hence, the motive for this work was to investigate the factors causing vibration problems in an inverted pendulum and an UAV (spring and damper coefficients) using Newton's fundamental analysis of motion (Euler equation). Therefore, this study expects to provide investigators with more information for proper comparison and methods for evaluating UAV's vibration and performance, as well as encouraging aeronautical engineers and academic investigators who are interested in studying vibrations, dynamic behaviors, and stabilization systems to consider all the missions to better understand the UAV's stability, which can be generalized in agricultural applications for the use of UAVs in agriculture spraying and crop aerial images to support precision farming.

MODELING METHODOLOGY AND PROCEDURES

Simulation methodology of the two systems

The two systems that were analyzed in this study are as follows: (1) an inverted pendulum (linearized only for small rotation angles, so that the system equation could be linear) and (2) a simple approximation of an aircraft wing subject to aerodynamic forces. Initially, the system used to carry out the simulation was the inverted pendulum system. The proposed model of an inverted pendulum was pivoted at one end, with double springs and viscous dampers attached at the halfway point of the pendulum rod (Figure 1).

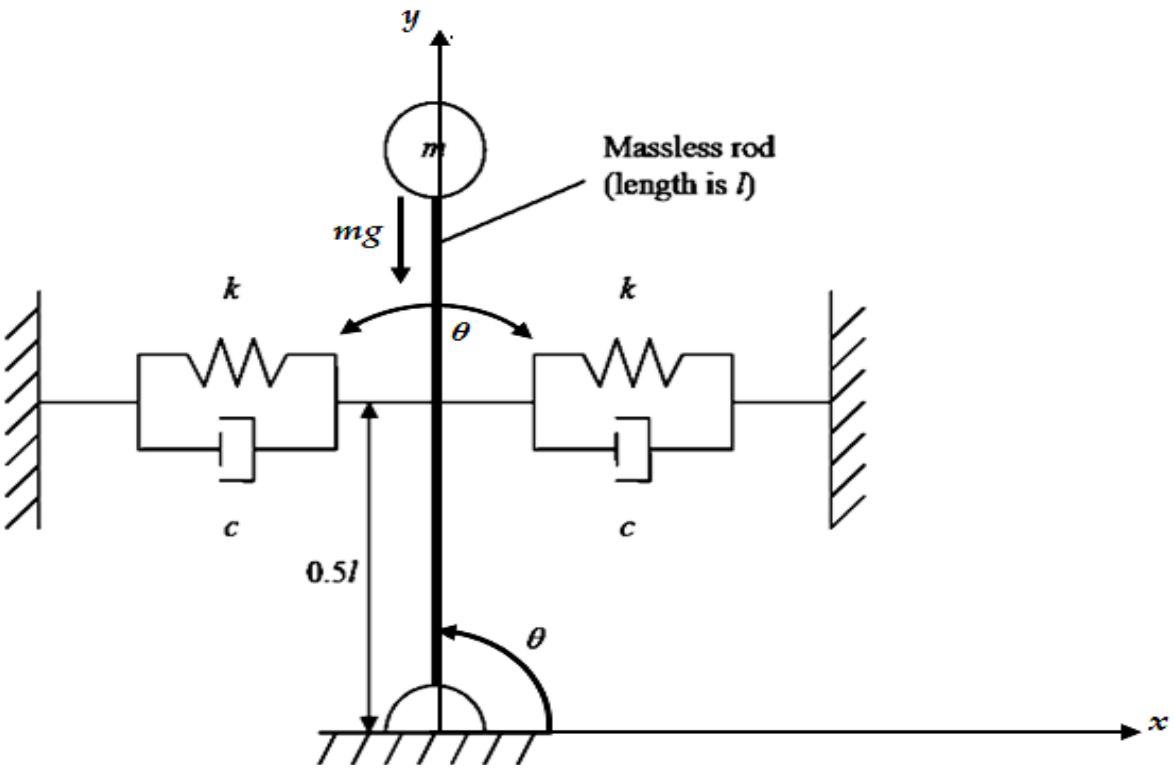

Figure 1. Diagram of the proposed dynamic model of an inverted pendulum with coupled springs and viscous dampers.

For the system of an inverted pendulum subject to aerodynamic forces, where the spring and damping combinations were located at the halfway point of the massless rod holding a small spherical mass m (0.5 kg), k is the spring's stiffness constant (32.69 N m^{-1}), c is the damping coefficient (1 N s m^{-1}), and θ is the angle through which the pendulum rotates (i.e., theta is the pendulum's angle from its vertical position (upward)). Proposed angular displacement (angle of the pendulum's rotation) θ = array of 2001 elements initialized to zero, and *l* is the length of the pendulum's rod (0.3 m) (Figure 1). Springs and viscous dampers are the mechanism of the pendulum pivoting rod for keeping the inverted pendulum moving horizontally until it reaches the vertical stability state.

The explanation of the UAV dynamic model parameters of the fuselage and wings is proposed to be the same as that of the dynamic model of the inverted pendulum machine with center pivot (Figure 1). The derivation of the motion equation and the natural frequency of the system were based on the mass of the pendulum, the length of the inverted pendulum. the stiffness of the springs, the damping coefficient required for the oscillations, with the oscillation reducing over time to zero, mass of the pendulum rod, and the initial angular displacement (in degrees). The acceleration of

the rod along its swing can be computed as the acceleration (motion) of the pendulum due to gravity, the direction, and the location of its head sphere, which is equal to some constant multiplied by the sine function. Consequently, Euler integration was used to carry out the project's time-domain simulation (Kelly, 2012; Russell, 2018; Garcia-Nieto *et al.*, 2019; The MathWorks Inc., 2022b). If a system with a generic single degree of freedom (SDOF) under free vibration is considered and Newton's law of motion is applied, the corresponding equation of motion is:

$$m\ddot{x} + c\dot{x} + kx = 0 \tag{1}$$

where $\ddot{x}$ is the system's acceleration (m s^{-2}), $\dot{x}$ is the velocity (m s^{-1}), x is the displacement (m) (i.e., the distance traveled by the mass), m is the pendulum's mass (kg), c is the damping coefficient (equivalent to the damping coefficient from combination of the two dampers, N s m^{-1}), and k is the spring's stiffness (equivalent to the stiffness from a combination of the two springs, N m^{-1}). The Euler integration was constructed from small time steps, *dt*. The acceleration of the current time step was determined by rearranging Equation (1) to yield the following expression for acceleration:

$$\ddot{x} = \frac{- c\dot{x} - kx}{m} \tag{2}$$

where the velocity and position can be obtained from the previous step; the initial conditions are used for the first step. The velocity for the current time step is determined by numerical Euler integration as:

$$\dot{x} = \dot{x} + \ddot{x}\, dt$$

where the velocity on the right-hand side of the equation is retained from the previous time step and is used to update the current value, and the acceleration multiplied by the time step *dt* is used to account for the increase in the velocity due to the acceleration of the system. The velocity from the left-hand side of the equation is then applied to determine the current displacement:

$$x = x + \dot{x}\, dt$$

The displacement on the right-hand side of the equation is retained from the previous time step, and the velocity multiplied by the time step *dt* is used to account for the increase in displacement due to the velocity of the dynamical system.
The value of the current acceleration is calculated in the following expression, which comes from the rearranged differential equation of motion of the inverted pendulum for θ, where θ is the pendulum angle (i.e., a second-order ordinary differential equation):

$$ml^2\ddot{\theta} + \frac{cl^2}{2}\dot{\theta} + \left(\frac{kl^2}{2} - mgl\right)\theta = 0 \quad (3)$$

The second part of the simulation was for the aircraft's wing. This process was based on a dynamic model derived by using the Euler approach, where Euler integration was used to estimate the response of an aircraft's wing section to aerodynamic forces. The behavior of the wing can be modeled by a single degree of freedom differential equation. The aerodynamic forces acting on the wings depend on the velocity. It is being assumed that this system did not have a constant velocity, so the acceleration occurred because of the variation in the aircraft's direction. This means that the equation of motion for the forcing term is:

$$m\ddot{x} + c\dot{x} + kx = \gamma\dot{x}$$

where γ (gamma) is the damping coefficient (N s m^{-1}) and $\gamma\dot{x}$ is the velocity-dependent effect of the aerodynamic forces on the wings (N) (i.e., a periodic propulsive force).

Intended procedures of the two systems

The two systems that needed to be activated were the inverted pendulum and a simple aircraft wing subject to aerodynamic forces, where the spring and damping combinations were located at the midpoint of the massless rod holding a small spherical mass m, k was the spring's stiffness constant, c the damping coefficient, θ the angle through which the pendulum rotated (i.e., theta was the pendulum angle from its vertical position (upwards)), l the length of the pendulum rod, and g was the constant gravitational acceleration (9.80665 m s^{-2}) (Figure 1). Therefore, an overall description of the MATLAB simulations for each system implemented in this study is presented in the following sections.

The inverted pendulum simulation process

MATLAB is widely used to implement simulations of various application models, such as simulating the behavior of a dynamic system. The unique advantage of using MATLAB is that this software can handle the time in milliseconds to develop and confirm the results of the algorithms. In the simulation of the inverted pendulum system, the user is first asked to input the simulation system they wish to run, as follows: 1 for the inverted pendulum system, and 2 for the aircraft wing system. If the choice is 1, several variables are initiated. The gravitational constant g is set to a value of 9.80665 m s^{-2}. The mass of the pendulum is set to 0.5 kg, the damping coefficient is set to 1 N s m^{-1}, and the length of the pendulum rod is set to 0.3 m.

Initially, the simulation calculates the value of the limiting spring's stiffness at the limit of stability (k_lim = 2 m g l^{-1}). The system displays the value of the calculated limiting stiffness, and the user is asked for the value of the multiplier of k_lim to be used as the

final variable. The k_value (spring stiffness) is the product of the multiplier and the calculated limiting spring's stiffness (k_lim). The final stiffness of the spring (k_value) is then displayed in units of N m^{-1}. Certain selected time steps were too large to carry out the simulation and were not considered in this study. Thus, the step size (*dt*), i.e., the step size in seconds, is then set to a value of 5 ms and the time is set to run from 0 s to 2000 step sizes, or 10 s, in steps of 5 ms. The variable theta (θ) is set as an array of 2001 elements initialized to zero. Theta_dot ($\dot{\theta}$), which is a variable representing the velocity of the center of mass (m) from the vertical position, is set to an array of 2001 elements initialized to zero. Theta_dbl_dot ($\ddot{\theta}$) is set to an array of 2001 elements initialized to zero, and this variable represents the acceleration of the center of mass (m) of the inverted pendulum as it swings. The following expression was used:

(θ_1) *theta* (1) = 5 * (*pi* / 180) + *theta* (1)

which is where the initial conditions of theta are set; the theta (θ, angle) on the left side is the current value of theta (angle) and is set to 5 ° in terms of radians plus the value of the first element in the theta array, which is zero.

The next expression is:

$(\dot{\theta}_1)$ *theta_dot* (1) = 0 + *theta_dot* (1)

which is where the initial conditions of velocity theta_dot are set; the velocity (theta_dot) on the left-hand side is the current value of velocity and is set to 0 (rad s^{-1}) plus the value of the first element in the velocity array, which is zero. Thus, the programming loop can start calculating the value of theta (*θ*, angular displacement) with respect to time, θ(t). The counter-variable, n, was set to run from 2 to 2001 in steps of 1. The value of the current acceleration ($\ddot{\theta}_n$) theta_dbl_dot(n) is calculated by the following expression (as written in MATLAB):

$(\ddot{\theta}_n)$ *theta_dbl_dot* (*n*) = - (((*c* * (l^2)/2) * *theta_dot* (*n*-1)) + (((*k_value* * (l^2)/2) - (*m* * *g* * *l*)) * *theta* (*n*-1))) / (*m* * (l^2))

which comes from the rearranged differential equation of motion of the inverted pendulum as shown in Equation 3.

The theta_dot(n-1) is the value of the velocity ($\dot{\theta}_{n-1}$) from the previous step, and theta(n-1) is the value of the theta for angular displacement (θ_{n-1}) from the previous step. The proposed equation assumes small angles (*θ*) (i.e., theta is varied between +5 and -5 °), so the system's equation is linear. The expression used to calculate the current value of velocity ($\dot{\theta}_n$) *theta_dot*(*n*) as written in MATLAB is: *theta_dot*(*n*) = *theta_dot*(*n*-1) + *theta_dbl_dot*(*n*) * *dt*, where *theta_dot*(*n*-1) is the value of the velocity from the previous step plus the current value of acceleration multiplied by the time step.

The expression used to calculate the current angular displacement (θ_n) theta(n) as written in MATLAB is:

theta(n) = *theta*(n-1) + *theta_dot*(n) * *dt*,

where theta(n-1) is the value of the pendulum's swing angle from the previous step plus the value of the current velocity multiplied by the time step. This is so the programming loop ends and the angle's theta (θ) is converted back to degrees. A plot of theta (angular displacement, θ) versus time is established with the time as the horizontal axis and the theta (θ, angular displacement) as the vertical axis. The boundaries of the plot are set as follows: the horizontal axis is set between 0 and 10 s and the vertical axis is set between -15 and 15 °. Finally, the simulation can be terminated by writing "End", and the inverted pendulum simulation ends.

The aircraft wing simulation process

In MATLAB, if the user selects Choice 2, the user wants to run the aircraft wing simulation, the aircraft wing simulation starts immediately. Several variables are initiated: the system's mass (m) is set to 500 kg, the spring's stiffness (k) is set to 1×10^7 N m^{-1}, and the aerodynamic effect on the system (i.e., gamma (γ)) is set to 1×10^4 N s m^{-1}. The damping coefficient at the limit of stability (c_lim) is set to equal to the value of gamma (γ), the calculated value of c_lim is then displayed in N s m^{-1}. The user is then asked to enter the desired multiplier value for the damping coefficient at the limit of stability (c_lim). The final value for the damping coefficient at the limit of stability is then set to c_value and is equal to the damping multiplier (c_multiplier) multiplied by the c_lim. The final calculated value of c_value (damping coefficient) is displayed in N s m^{-1}. The time step (dt) is set to 0.002 s and the time is initially set to be between 0 and 2500 step sizes, or 5 s. The displacement (x), velocity x_dot ($\dot{x}$), and acceleration x_dbl_dot ($\ddot{x}$) are each set to an array of 2501 elements initialized at zero.

The expression (x_1), $x(1) = 1 + x(1)$ is where the initial conditions of the displacement (x) are set, where the x on the left side is the current value of x and is set to 1 mm plus the value of the first element in the x array, which is zero. The next expression as written in MATLAB is ($\dot{x}_1$), $x\_dot(1) = 0 + x\_dot(1)$, which is where the initial conditions of the velocity $\dot{x}$ (x_dot) are set; the x_dot on the left-hand side is the current value of x_dot and is set to 0 mms^{-1} plus the value of the first element in the x_dot array, which is zero. Thus, the programming loop can be started to calculate the value of the displacement (x) with respect to time, $x(t)$. The counter-variable, n, is set to run from 2 to 2501 in steps of 1.

The mathematical expression used to calculate the acceleration ($\ddot{x}$), x_dbl_dot, as written in MATLAB is:

x_dbl_dot (n) = - (((*c_value - gamma)* * (*x_dot* (n-1)) + ((*k*) * *x* (n - 1))) / *m*)

which is derived from the rearranged equation of motion of the aircraft wing (Equation 2). The expression used to calculate the current value of velocity ($\dot{x}_n$), x_dot(n), as written in MATLAB is:

$$x\_dot\ (n) = x\_dot\ (n\text{-}1) + x\_dbl\_dot\ (n) * dt$$

where ($\dot{x}_{n\text{-}1}$) x_dot(n-1) is the value of velocity from the previous step plus the current value of acceleration multiplied by the time step. Likewise, the expression used to calculate the current value of displacement, x(n) as written in MATLAB is:

$$x(n) = x\ (n\text{-}1) + x\_dot\ (n) * dt$$

where $x(n\text{-}1)$ is the value of displacement from the previous step plus the current value of velocity multiplied by the time step. The loop of the programming circuit ends, and the plot of displacement x versus time is established. The boundaries of the plot are set as follows: the horizontal axis limit is set between 0 and 5 s and the vertical axis limit is set between -5 and +5 mm. Finally, the simulation can be terminated by writing "End", so the aircraft wing simulator ends.

RESULTS AND DISCUSSION

To clarify the performance of the proposed inverted pendulum, a numerical simulation was carried out using MATLAB software based on the physical parameters of the pendulum system, which were set. In the inverted pendulum simulation system, the initial results found the spring's stiffness at the limit of stability k_{lim} = 32.69 N m^{-1}, then the time-domain simulation was programmed to determine the angular displacement (rotation (θ)) as a function of time.

Before running the time domain simulations for the two systems, the limiting coefficients of the springs and viscous dampers of the two systems (spring's stiffness k_{lim} and damping coefficient c_{lim}) need to be manually calculated. The limiting factor for the inverted pendulum was considered to be the spring's stiffness at the limit of stability, k_{lim}. The calculation was as follows:

$$k\left(\frac{2mg}{l}\right)\text{lim} = k\left(\frac{2(0.5\ kg)\ (9.807\ ms^{-2}}{0.3\ m}\right)\text{lim} = 32.69\ N\ m^{-1}$$

When the value of k_{lim} (32.69 N m^{-1}) was used, the time-domain simulation for the inverted pendulum could be run for various values of stiffness (k) to obtain the rotation angle (θ). An inverted pendulum with an affected force (mechanical energy) has an initial position of theta > 0 ° at t = 0 s (Figure 2).

The behavior of an inverted pendulum (Figures 2-4) showed its response is evident at different values of stiffness (k_{lim}) when the simulation was run at 0.1, 0.5, 0.9, 0.99, 1, 5, and 10 k_{lim}. The angular displacement of the moving inverted pendulum mass

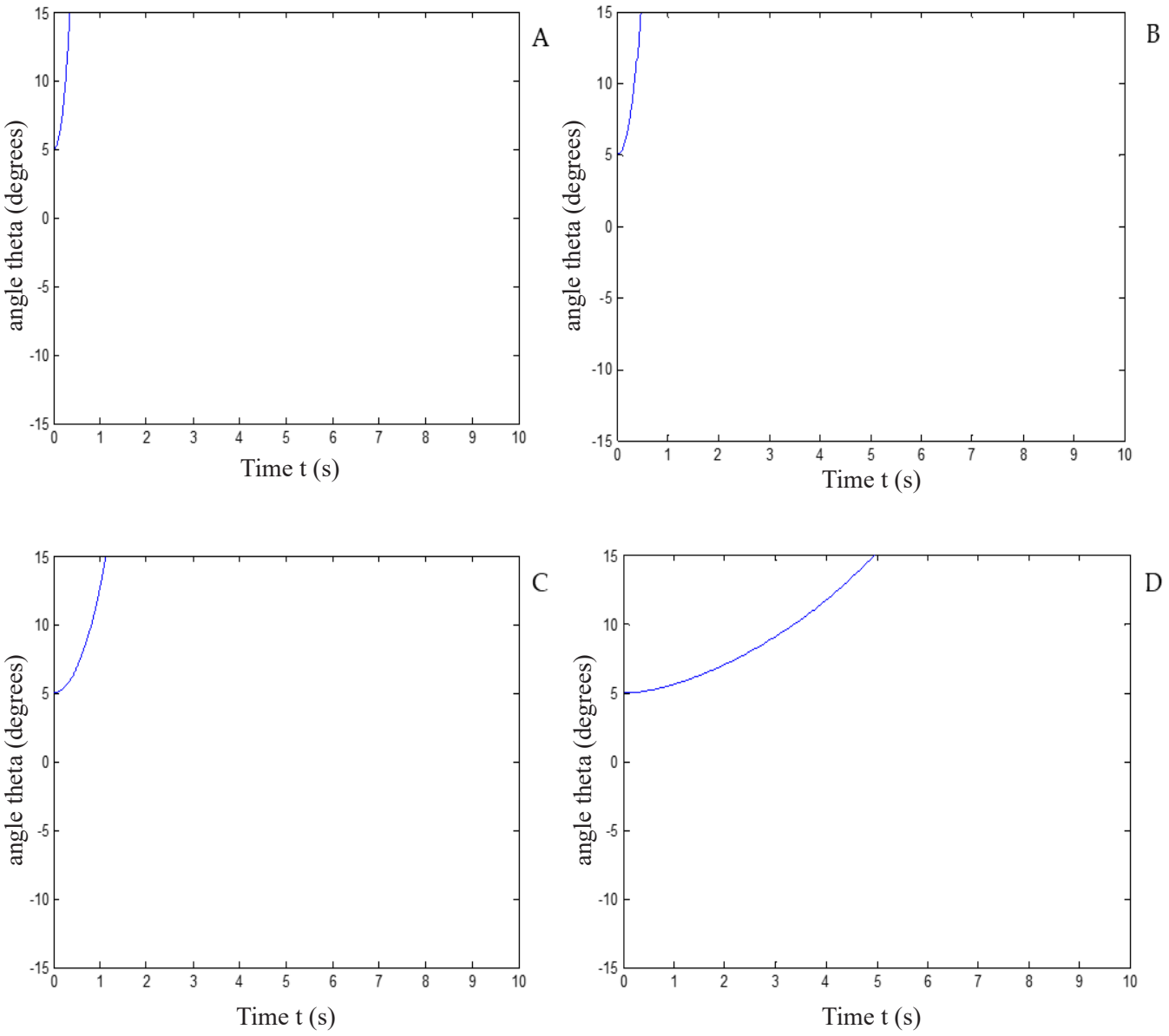

Figure 2. Angular displacement θ, with rotation at different levels of spring's stiffness k_{lim} (nonideal step response). A: rotation at 0.1 k_{lim}; B: rotation at 0.5 k_{lim}; C: rotation at 0.9 k_{lim}; D: rotation at 0.99 k_{lim}.

was considered to be a function of time. The response of the pendulum model (Figure 2) clearly depicts the instability of the system with different levels of stiffness (k_{lim}), namely 0.1, 0.5, 0.9, and 0.99 k_{lim}. With the proper optimal spring stiffness (k), the system's state stabilized within a few seconds. The same responses were studied with different initial conditions (0.087 rad (≈ 0.1 rad) for angle) (Figures 2 and 3). Further

simulations were run with a step disturbance (Figure 4), and the proposed optimal controller was able to stabilize the system successfully.

As seen in the figures, the function describing the rotation angle varied greatly when the value of k was changed. Unfortunately, for values of k less than k_{lim}, the system displayed divergent instability and immediately deviated sharply from the mean without stabilizing. In the model, this would represent the case where the inverted pendulum moved all the way to one side and stayed there without being able to stabilize itself about the mean angle.

The output of the pendulum's vibration was where the system was able to stabilize the pendulum in 7 s (Figure 4B). The swinging stabilization system had a number of decreasing swings before the pendulum reached a vertical position. The angular displacement of the pendulum deviated to a maximum of 5 ° when the vibration was introduced, but the swinging stabilization system was able to reduce the oscillation in less than 8 s, which made the pendulum maintain its upright position. For values of k greater than k_{lim}, the system displayed asymptotic stability. The rotation angle approached an equilibrium position of θ = 0 °, with the magnitude of vibrations decreasing over time. This means that the pendulum could reach the vertical position (θ = 0 °); however, with parameters set (at the ideal step response of 10 k_{lim}), the time the system takes to reach stability is important (in 7 s).

In the particular case where the stiffness was equal to the limiting stiffness ($k = k_{lim}$), the system displayed stable behavior. The rotation angle in this case remained at the initial value without deviation over time. This could be seen when k_{lim} was entered as the value of k in the original differential equation (with an initial displacement (θ) of 5 ° and an initial velocity ($\dot{\theta}$) of zero), as in the following formulae:

$$k = k\left(\frac{2mg}{l}\right)\lim$$

$$ml^2\ddot{\theta} + \frac{cl^2}{2}\dot{\theta} + \left(\frac{kl^2}{2} - mgl\right)\theta = 0$$

$$ml^2\ddot{\theta} + \frac{cl^2}{2}\dot{\theta} + \left(\frac{\frac{2mg}{l}l^2}{2} - (mgl)\right)\theta = 0$$

$$ml^2\ddot{\theta} + \frac{cl^2}{2}\dot{\theta} + (0)\theta = 0$$

$$ml^2\ddot{\theta} + \frac{cl^2}{2}(0) + (0)(5°) = 0$$

$$ml^2\ddot{\theta} = 0$$

$$So, \ddot{\theta} = 0$$

In this case, no vibratory motion occurred, and the system remained at the initial displacement angle. This makes sense because of the small angle assumption made at the start of the process (Sin (0) ≈ 0 and Cos (0) ≈ 1). In general, the figures illustrate that the angle and position of the pendulum system can provide an acceptable response since the initial condition of θ = 5 ° was not large. The initial displacement angle at time t = 0 s for this system was 5 °. The pendulum's response shows that for a unit step actuated by a force, the system was unstable, and a settling time of 7 s was achieved

by increasing the value of the spring's stiffness, k. In the beginning, with a small value of stiffness k, there was a small amount of oscillation, but it took an unacceptably long time to reach the steady state. The result of theta rotation (θ) versus time (t) at different levels of limiting the spring's stiffness (5 and 10 k_{lim}) is shown (Figure 4). It is clear that for 10 k_{lim}, the pendulum's position became almost stable in a short settling time (7 s). In addition, for the second system, to clarify the performance of the proposed simple aircraft wing subject to aerodynamic forces, a numerical simulation was carried out using MATLAB software based on the parameters of the wing system that were set. Furthermore, as shown in the simulation figures, the displacement of the moving system's mass was considered to be a function of time. For the system analysis, in the case of self-excited vibration (flutter), the factor limiting the motion was the damping coefficient at the limit of stability (c_{lim}). This is because the aerodynamic forces on the wing are velocity-dependent (similar to the damping force), feeding back into the differential equation of motion and thus affecting the stability of the system.

The limit of stability occurs when the damping ratio (ζ, dimensionless) reaches zero ($\zeta = 0$), meaning the damping coefficient at the limit of stability (c_{lim}) can be calculated as follows:

$$\zeta = \frac{(c - \gamma)}{2\sqrt{km}} = 0$$

$$c_{\lim} = \gamma$$

$$S_o,\ c_{\lim} = 1 \times 10^4\ N\ s\ m^{-1}$$

Using this value for c_{lim} (10 000 N s m^{-1}), the simulation for the aircraft wing was run for various values of the damping coefficient (c) to determine the wing's position (displacement x) as a function of time (t) and implemented by using the Euler Method. Therefore, the simulation's output results for different values of the damping coefficient (c), namely 0.5, 0.9, 0.99, 1, 1.1, and 2 c_{lim}, show the displacement response of the moving system's mass (x) versus time (t) (Figure 5).

The model's response shows that for the 0.5 and 0.9 c_{lim} damping coefficients, the instability of the system showed a clear periodic oscillation (Figure 5). Moreover, the displacement amplitude of the system's oscillations and the period of oscillations increased with time. Furthermore, a negative dynamic stability (dynamically unstable, with divergent oscillation) at damping coefficients at limits of stability (c_{lim}) of 0.5, 0.9, and 0.99 c_{lim} (i.e., the disturbance caused a magnification of the amplitude over time) was found (Figures 5A, 5B, and 5C). An undamped oscillation (a neutral dynamic system) was obtained at 1 c_{lim} (Figure 5D). The results also show that as the damping coefficient increased with time, the displacement amplitude of the oscillations decreased, but the period of the oscillations was still at the increasing limit (Figures 5A–5D). The system was under damped oscillation (dynamically stable, called a positive dynamic system in a stable equilibrium position) when the damping coefficient at the limit of stability (c_{lim}) was 1.1 and 2 c_{lim} (Figures 5E and 5F). In general, as only applied

to this study, for the flight of an aircraft to be stable, the results of the oscillation must be damped immediately, and this can be achieved by increasing the value of the damping coefficient (c).

Moreover, as seen from the simulation figures, the stability of the aircraft wing was dramatically affected by changes in the damping coefficient (which relate to a change in the damping ratio ζ of the system). For values of c less than c_{lim}, the damping ratio, ζ, will be negative. In these cases, the system will be unstable and will show an exponential rise due to underdamping (i.e., disturbance over time). This can be seen in the first four cases (Figures 5A–5D), where the damping coefficient (c) was less than the damping coefficient at the limit of stability (c_{lim}). However, for the cases where c was greater than c_{lim}, the system (Figures 5E and 5F) exhibited stable behavior (or asymptotically stable behavior, as ζ < 1 for the given cases). The displacement rapidly approached the equilibrium position of 0 mm as time (t) increased. In addition, in the particular case where c = c_{lim} (Figure 5E), the airplane wing displays what is known as marginal stability (in 3.5 s). This is because the damping ratio ζ of the system was equal to zero, as shown by:

$$c = c_{\text{lim}} = \gamma$$
$$\zeta = \frac{(c - \gamma)}{2\sqrt{km}} = \frac{(\gamma - \gamma)}{2\sqrt{km}} = 0$$
$$S_o, \zeta = 0$$

According to this result, if the damping ratio (ζ) is equal to zero, the system will vibrate consistently at its natural frequency of oscillation (w_n), i.e., for a zero-damping effect, it will never deviate so drastically as to become unstable, but it will never stabilize at a final value. Significantly, one can observe in the figures that the displacement of the moving system mass and the position of the aircraft wing system as simulated in the MATLAB experiment showed a satisfactory response.

For the inverted pendulum (Figures 2–4), the critical angular displacement (θ) versus time (t) measured by simulation of the pendulum's vibration for different levels of the spring's stiffness k_{lim}, demonstrated that the system contained the positive characteristics of the equation of motion and that its step response to the inputs could also increase to infinity (i.e., an unbounded response), and thus the angle θ could increase infinitely (Figure 2). In this case, the k_{lim} command can be utilized to simulate the response of the angular displacement θ of the pendulum model to random inputs. The result confirmed that the response of the pendulum system to a step input with slow oscillation was unstable around the vertical position (Monir, 2018); however, the pendulum could become stable in its inverted position (i.e., the inverted pendulum can eventually reach the vertical equilibrium position) if the pendulum oscillates at a constant velocity, or the inverted pendulum will stabilize at an angle (the stability angle of the inverted position). It can be seen that the pendulum swung until it settled at θ = 5 ° (the angle of stability) (Figure 3). Additionally, the pendulum remained in

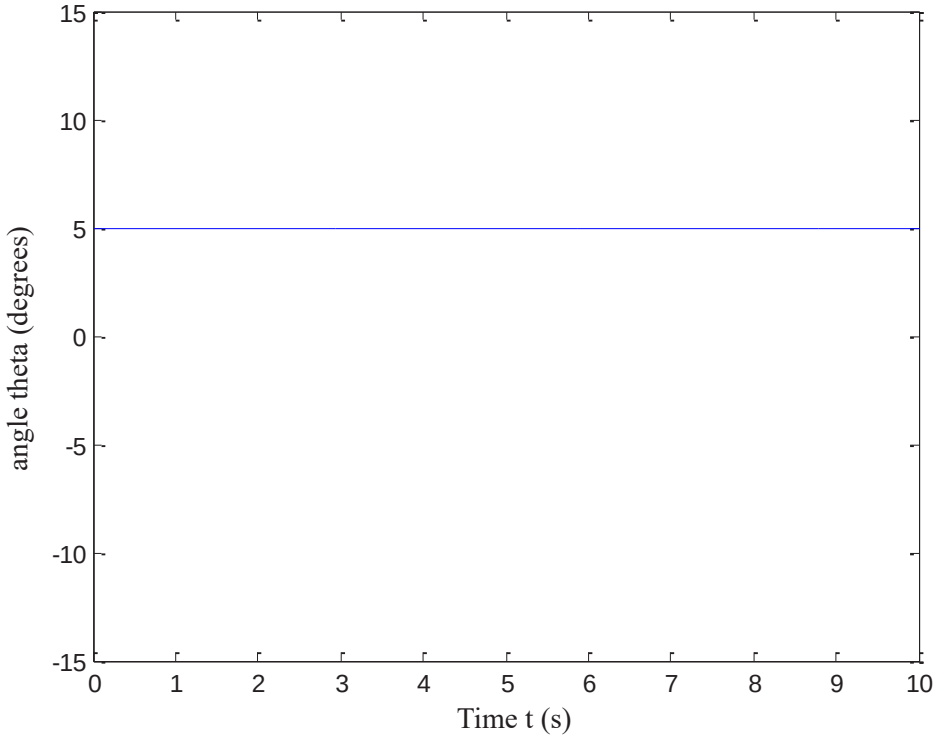

Figure 3. Angular displacement θ, with rotation at spring's stiffness 1 k_{lim} (neutral position).

an upright position with rapid oscillation, and the pendulum's oscillation around the vertical position remained small. Thus, with fast oscillation, in which the initial oscillation amplitude of the inverted pendulum was 5 °, the pendulum could be kept stable around its vertical position (Figures 4A and 4B), and the pendulum swung at θ = 5 ° until it settled at θ = 0 ° in 7 s.

Over time, the angular amplitude of the oscillations decreased, but the period of the oscillations was still at the increasing limit (Figure 4A). Fluttering was dampened in about 7 s (Figure 4B), when the value of the spring's stiffness was about 10 k_{lim}. In general, the results show that the inverted pendulum can be kept vertical within 5 ° when controlled by using different spring displacements k, and that when the pendulum is in the vertical position (θ = 0 °), the springs do not extend. In these figures, it is obvious that the amplitude of vibration decayed over time. The simulation results demonstrated that the lateral angular (angular rotation) response of the inverted pendulum, which showed a normal vibration with different values of the spring coefficient (k), had a very small settling time with increased spring coefficient (k) values, which efficiently brought the pendulum to the inverted position (i.e., upswing). The method of analyzing the aerodynamics that affect the aircraft can be used to analyze the stability and flight control of UAVs. This can be accomplished by comparing

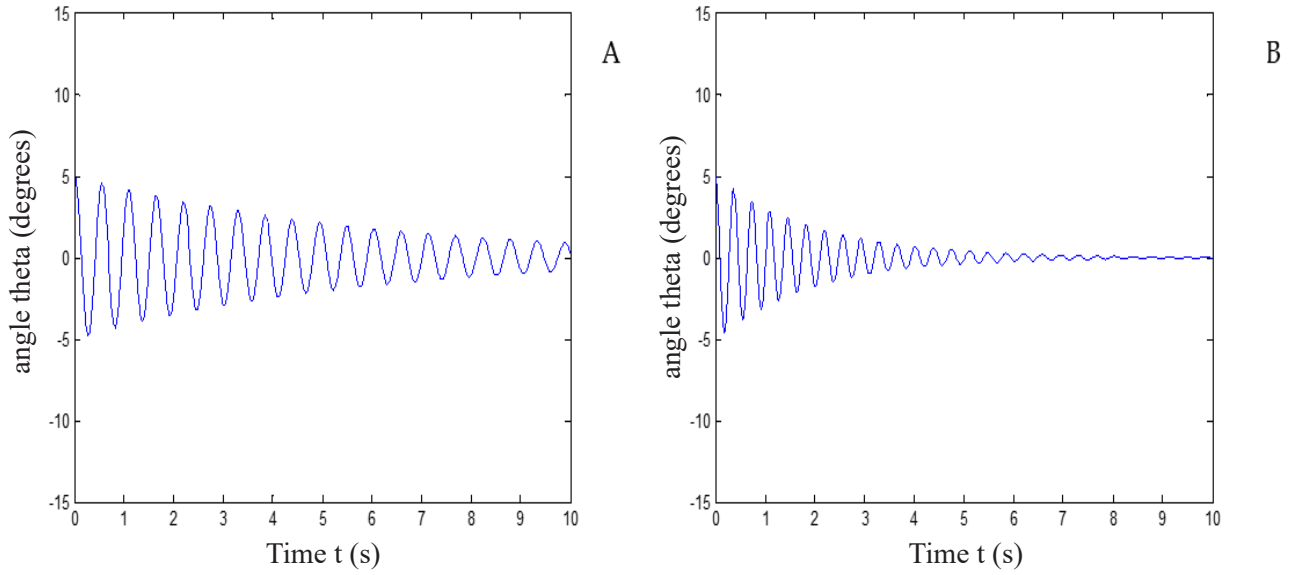

Figure 4. Angular displacement θ, with rotation at different levels of spring's stiffness k_{lim} (ideal step response). A: rotation at 5 k_{lim}; B: rotation at 10 k_{lim}.

the stability of an inverted pendulum system to the wings of an uncrewed aircraft. Accordingly, there are some noticeable aerodynamic forces that affect a UAVs' flight: thrust, drag, lift, weight, and the coefficients of pitch moment and attack angle (FAA, 2016). Furthermore, from the perspective of an aircraft wing subject to aerodynamic forces, the displacement of the moving system's mass (mm) versus time (seconds) when the simulated values of the damping coefficient c increased, namely 0.5, 0.9, 0.99, 1, 1.1, and 2 c_{lim}, reflected a stable system (Figures 5A–5F).

For the aircraft wing (Figure 5), the initial displacement at time t = 0 s for this system was 1 mm. The initial displacement response of the moving system's mass (x) varied between +5 and -5 mm at the lowest damping coefficients (c) at the limit of stability. With increasingly higher coefficients, the displacement decreased to the initial displacement limit between +1 and -1 mm. The time-domain responses in displacement of the moving system's mass for the two highest values of the damping coefficient c (the damping coefficient at the limit of stability), namely 1.1 and 2 c_{lim}, showed the minimum amplitude of the mass displacement of this system and the least time required for the system to reach stability (Figures 5E and 5F). This illustrated greater responsiveness to relatively rapid changes in state and thus represented the most efficient flight path.

In addition, the results showed that with time, the displacement amplitude of the oscillations decreased and the period of the oscillations also decreased (Figures 5E and 5F). Therefore, to stabilize the flight, the oscillation was completely damped after a certain time period. Finally, the originally proposed equivalent viscous damping ratio

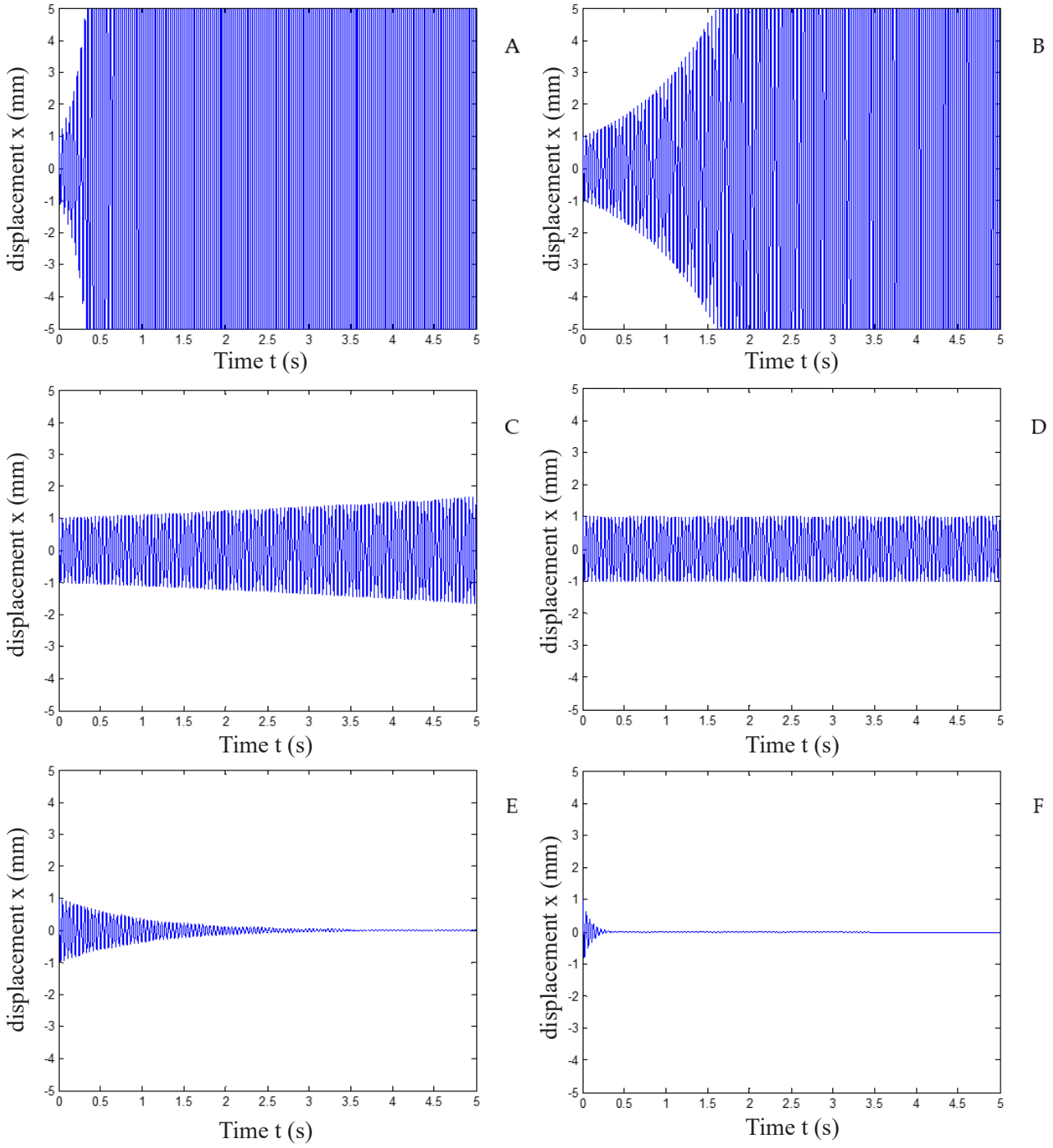

Figure 5. Displacement response of the moving system's mass at different values of damping coefficient c_{lim}. A: response at 0.5 c_{lim}; B: response at 0.9 c_{lim}; C: response at 0.99 c_{lim}; D: response at 1 c_{lim}; E: response at 1.1 c_{lim}; F: response at 2 c_{lim}.

was 0 % ($\zeta < 1$), with the displacement amplitude ranging from less than 1 to 5 mm, according to the Euler method. The time taken to reduce the displacement amplitude from 5 mm to less than 1 mm was reduced from about 5 s to 400 ms. The results show that a damping coefficient of more than 10,000 N s m^{-1} was more effective. The aircraft took a very short time to return to its reference condition and was kept at a certain rotation angle (i.e., the aircraft took off in an accurate and stable position).

This system gave an actual time response with a relatively small magnitude of oscillation, since the figures clearly show that the amplitude of oscillation decayed over time more quickly, thus achieving the objective of designing effective aircraft wings. There was only a small degree of oscillation for 400 ms (Figure 5F). For a system controlled by the damping coefficient, the system's model is more responsive to relatively fast alterations in its state induced by aerodynamic forces, and so the model of a dynamic system will therefore be faster to reach a steady-state position and to respond to disturbances than a system with a poorly-tuned damping coefficient or one in which the dynamic system has not achieved damping control. In addition, these results also show that the flight instability of UAV aircraft during the turbulence associated with takeoff and the subsequently delayed flight stability were more pronounced than that of flight at higher airspeeds, and significant stability disturbances could be caused by the action of small external forces on the aircraft's propellers or the aircraft itself. Inefficiencies in the flight control systems can also be a problem for stable operations.

Recently, UAVs have been widely applied in agriculture, especially for operations in precision agriculture (PA) (Radoglou-Grammatikis *et al.*, 2020; Wang *et al.*, 2021), which require a highly efficient aircraft control system. Therefore, modern automated control systems have been applied in many areas, but are of particular importance in flight operations. The elements of the control system need to be clearly understood, and the basic concepts of controllers need to be developed to maintain stability while reacting to external forces, such as unexpected vibration on the uncrewed aircraft's structure or the multirotor aircraft arms (rotary wings) that operate almost autonomously, which may indicate the presence of external noise entering the UAV's control systems, typically caused by sequential excitation of aerodynamic or atmospheric air turbulence (i.e., external sources) (Al-Mashhadani, 2018, 2019; Ghazali and Rahiman, 2022).

CONCLUSIONS

This research indicated that for the establishment of flight stability, the first dynamic moments of flight in an uncrewed aerial vehicle (UAV) and its response to any surrounding disturbances are the most significant. The findings from the simulation of the inverted pendulum showed that as the value of the spring's stiffness at the limit of stability, k_{lim}, increased, the system became more convergent and, as a result, more stable. The system vibrated consistently at its natural frequency (w_n), never deviating drastically to become unstable, but also never stabilizing at a final value. The simulated inverted pendulum's displacement versus time showed that the inverted pendulum could become stable despite the slightly periodic oscillation with an increase in the

value of the spring coefficient. The aircraft system displayed stable behavior with an increase in the value of the damping coefficient. The displacement amplitude of the system's oscillations, as well as the period of the oscillations, increased with time when the damping coefficient was below a certain value. These results would significantly help in creating a clear and understandable path for improving the implementation of UAVs in agricultural field operations, especially with an additional payload, which may affect the center of gravity of the UAV and its flight stability.

ACKNOWLEDGEMENTS

The authors of this study would like to express their appreciation to the University of Florida, and the Deanship of Scientific Research, Researchers Support Services Unit, Agriculture Research Center, and College of Food and Agriculture Sciences at the King Saud University for their support and encouragement.

REFERENCES

Al-Mashhadani MA. 2018. Random vibrations in unmanned aerial vehicles, mathematical analysis and control based on expectation and probability. Journal of Low Frequency Noise, Vibration and Active Control 38 (1): 143–153. https://doi.org/10.1177/1461348418813031

Al-Mashhadani MA. 2019. Optimal control and state estimation for unmanned aerial vehicle under random vibration and uncertainty. Measurement and Control 52 (9–10): 1264–1271. https://doi.org/10.1177/0020294019866860

Bietresato M, Mazzetto F. 2019. Definition of the layout for a new facility to test the static and dynamic stability of agricultural vehicles operating on sloping grounds. Applied Sciences 9 (19): 4135. https://doi.org/10.3390/app9194135

Dolatabad MR, Pasharavesh A, Khayyat AAA. 2022. Analytical and experimental analyses of nonlinear vibrations in a rotary inverted pendulum. Nonlinear Dynamics 107 (3): 1887–1902. https://doi.org/10.1007/s11071-021-06969-0

Estevez J, Lopez-Guede JM, Garate G, Graña M. 2021. A hybrid control approach for the swing free transportation of a double pendulum with a quadrotor. Applied Sciences 11 (12): 5487. https://doi.org/10.3390/app11125487

FAA (Federal Aviation Administration). 2016. Pilot's handbook of aeronautical knowledge, Chapter 5: Aerodynamics of Flight. Oklahoma City, OK, USA. https://www.faa.gov/regulations_policies/handbooks_manuals/aviation/phak (Retrieved: June 2022).

Fabbri A, Molari G. 2004. Static measurement of the centre of gravity height on narrow-track agricultural tractors. Biosystems Engineering 87 (3): 299–304. https://doi.org/10.1016/j.biosystemseng.2003.12.008

Garcia-Nieto S, Velasco-Carrau J, Paredes-Valles F, Salcedo JV, Simarro R. 2019. Motion equations and attitude control in the vertical flight of a VTOL bi-rotor UAV. Electronics 8 (2): 208. https://doi.org/10.3390/electronics8020208

Gatto A. 2009. Application of a pendulum support test rig for aircraft stability derivative estimation. Journal of Aircraft 46 (3): 927–934. https://doi.org/10.2514/1.38916

Ghazali MHM, Rahiman W. 2022. Vibration-based fault detection in drone using artificial intelligence. IEEE Sensors Journal 22 (9): 8439–8448. https://doi.org/10.1109/jsen.2022.3163401

Gunawan WW, Likafia A, Joelianto E, Widyotriatmo A. 2018. Inverted pendulum stabilization with flying quadrotor. Internetworking Indonesia Journal 10 (2): 29–35.

Hanada H, Asari K, Tsuruta S, Araki H, Funazaki K, Satoh A, Taniguchi H, Kikuchi M. 2019. Experiments of inverted pendulum as a vertical reference of a telescope. Journal of Physics: Conference Series 1301 (1): 012013. https://doi.org/10.1088/1742-6596/1301/1/012013

Jibril M, Tadese M, Tadese EA. 2021. Stability control of a rotational inverted pendulum using augmentations with weighting functions based robust control system. Researcher 13 (1): 17–21. https://doi.org/10.7537/marsrsj130121.03

Kelly SG. 2012. Mechanical vibrations: Theory and applications. Cengage Learning: Stamford, CT, USA. 898 p.

Khorsandi F, Ayers PD, Freeland RS, Wang X. 2018. Modeling the effect of liquid movement on the center of gravity calculation of agricultural vehicles. Journal of Terramechanics 75: 37–48. https://doi.org/10.1016/j.jterra.2017.09.005

Li L, Xie Z, Luo X, Li J. 2021. Trajectory planning of flexible walking for biped robots using linear inverted pendulum model and linear pendulum model. Sensors 21 (4): 1082. https://doi.org/10.3390/s21041082

The MathWorks Inc. 2022a. MATLAB version: 9.13.0 (R2022b). The MathWorks Inc. Natick, MA, USA. https://www.mathworks.com

The MathWorks Inc. 2022b. Help center: Simulate the motion of the periodic swing of a pendulum. The MathWorks Inc. Natick, MA, USA. https://www.mathworks.com

Monir M. 2018. Analyzing and designing control system for an inverted pendulum on a cart. European Scientific Journal 14 (6): 387–398. https://doi.org/10.19044/esj.2018.v14n6p387

Radoglou-Grammatikis P, Sarigiannidis P, Lagkas T, Moscholios I. 2020. A compilation of UAV applications for precision agriculture. Computer Netwworks 172: 107148. https://doi.org/10.1016/j.comnet.2020.107148

Russell DA. 2018. Acoustics and vibration animations: Oscillation of a simple pendulum. The Pennsylvania State University: University Park, PA, USA. https://www.acs.psu.edu/drussell/Demos/Pendulum/Pendulum.html (Retrieved: June, 2022).

Sharma S, Sharma R, Kumar V, Chandel S. 2021. Analysis of a tiltrotor vertical take-off and landing unmanned aerial vehicle: CFD approach. IOP conference series: Materials Science and Engineering 1116 (1): 012096. https://doi.org/10.1088/1757-899x/1116/1/012096

Sowjanya R, Ramesh G. 2015. Design of optimal controller for double inverted pendulum. International Journal of Emerging Engineering Science and Technology 1 (5): 261–265.

Tulapurkara EG. 2012. Flight dynamics II - Airplane stability and control, IIT Madras. National Programme on Technology Enhanced Learning: Chennai, India. https://nptel.ac.in/courses/101106043 (Retrieved: July, 2022).

University of Michigan. 1997. Control tutorials for matlab. Ann Arbor, MI, USA. https://www3.diism.unisi.it/~control/ctm/examples/pend/invSS.html (Retrieved: July, 2022).

Wang X, Zhang X, Gong H, Jiang J, Rai HM. 2021. A flight control method for unmanned aerial vehicles based on vibration suppression. IET Collaborative Intelligent Manufacturing 3 (3): 252–261. https://doi.org/10.1049/cim2.12027